Model-Aided Inertial Navigation for Underwater Vehicles

Øyvind Hegrenæs, Einar Berglund, Oddvar Hallingstad

Abstract— **This paper reports the development and experimental evaluation of a complete model-aided inertial navigation system (INS) for underwater vehicles. The navigation system is novel in that accurate knowledge of the vehicle dynamics is utilized for aiding the INS, and the performance is evaluated using real data collected by an autonomous underwater vehicle (AUV). Together with real-time sea current estimation, the output from a kinetic vehicle model describing the dynamics is integrated in the navigation system. The presented experimental results verify that with merely an addition of software and no added instrumentation, it is possible to significantly improve the accuracy and robustness of an INS by utilizing the physical insight provided by a kinetic vehicle model. To the best of our knowledge, this paper is the first report on the implementation and experimental evaluation of a complete model-aided INS for underwater vehicle navigation. The proposed approach shows promise to improve underwater navigation capabilities both for systems lacking disparate velocity measurements, typically from a Doppler velocity log (DVL), and for systems where the need for redundancy and integrity is important, e.g. during sensor dropouts or failures, or in case of emergency navigation. The reported methodology is applicable to a large group of submersibles, as well as land and aerial crafts and robots.**

I. Introduction

A typical navigation sensor outfit for an underwater vehicle may consist of standard components such as compass, pressure sensor, and some class of inertial navigation system (INS). In addition, various sources of position aiding may be available, for instance long baseline (LBL) or ultra short baseline (USBL) acoustics, terrain-based techniques, and surface GPS. For an extensive survey on sensors and sensor systems, the reader should refer to [1] and references therein.

In practice, a submersible does not have continuous position updates, hence a navigation system based on INS, and especially low-cost INS, will have an unacceptable position error drift without sufficient aiding. While most high-end systems incorporate a Doppler velocity log (DVL) in order to limit the drift [1], [2], [3], [4], this additional expense is not always feasible. Even when a DVL is included, situations will occur where it fails to work or measurements are discarded due to decreased quality. In either case, in the absence of DVL measurements, alternative velocity information is required to achieve an acceptable low drift navigation solution between position updates. One possibility is to utilize mathematical models describing the vehicle dynamics, in conjunction with real-time sea current estimation.

Ø. Hegrenæs and O. Hallingstad are with the Department of Engineering Cybernetics, Norwegian University of Science and Technology, NO-7491 Trondheim, Norway. E-mail: hegrenas@unik.no; oh@unik.no.

E. Berglund is with the Norwegian Defence Research Establishment, NO-2027 Kjeller, Norway. E-mail: einar.berglund@ffi.no

The first author gratefully acknowledges the support of the Norwegian Research Council, Kongsberg Maritime, and Kongsberg Defence & Aerospace.

To date, the application of state estimators to underwater navigation has primarily focused on employing purely kinematic plant models, i.e. models describing the vehicle motion without the consideration of the forces and moments causing it [5], [6]. State estimators incorporating kinetic underwater vehicle models are rare. Model-based deterministic observers utilizing knowledge of the vehicle dynamics together with disparate measurements are reported in [7], [8]. As for work on model-aided INS, where the output from a kinetic vehicle model is used to aid the INS, the literature is scarce. Some reports are found related to aerial vehicles, where the navigation performance is assessed in simulation [9], [10], [11]. To the best of our knowledge however, no results have been reported on the implementation and experimental evaluation of a complete model-aided INS, nor has its practical application to underwater vehicle navigation.

In this paper, an aided INS also incorporating velocity measurements from a kinetic vehicle model is investigated. The proposed methodology, which is applicable to a large group of marine, land and aerial crafts and robots, is applied to underwater vehicle navigation, and the performance is experimentally evaluated using real data collected by an autonomous underwater vehicle (AUV). Preliminary experimental results have only recently been reported in [12]. This paper gives a further analysis and extends these results in that the navigation system Kalman filter (KF) accommodates simultaneous estimation of vehicle model output error and sea current. The enhanced KF also permits process and measurement noise level switching, e.g. varying sensor quality.

The remainder of this paper is organized as follows. Section II presents the mathematical vehicle model utilized in this paper. The integrated navigation system with model-aiding included is described in Section III. Section IV presents the experimental setup and experimental results.

II. Underwater Vehicle Modeling

Modeling of underwater vehicles is fairly complicated, and even when considered as a rigid body, an exact analysis is only possible by including the underlying infinite-dimensional dynamics of the surrounding fluid. While this can be done using partial differential equations, it still involves a formidable computational burden, infeasible for most practical applications. As a result, the conventional approach has been to use finite-dimensional approximations.

The development and experimental validation of the finite-dimensional kinetic vehicle model utilized in this paper have been rigorously treated in [13]. The main results are presented in the following. For a review and historical recap of work related to modeling of underwater vehicles, the reader should refer to the same paper and references therein.

TABLE I

NOMENCLATURE

Description	Variable	Entries*
Local Cartesian vehicle position	$\boldsymbol{p}^m_{mb}$	(x, y, z)
Earth-relative linear velocity	$\boldsymbol{v}^b_{mb} = \boldsymbol{v}^b_{eb}$	(u, v, w)
Water-relative linear velocity	$\boldsymbol{v}^b_{wb}$	(u_r, v_r, w_r)
Current velocity in body frame	$\boldsymbol{v}^b_{mw} = \boldsymbol{v}^b_{ew}$	(u_c, v_c, w_c)
Current velocity	$\boldsymbol{v}^l_{mw} = \boldsymbol{v}^l_{ew}$	(u^l_c, v^l_c, w^l_c)
Vehicle angular velocity	$\boldsymbol{\omega}^b_{mb} = \boldsymbol{\omega}^b_{eb}$	(p, q, r)
Attitude (roll, pitch, yaw)	$\boldsymbol{\Theta}$	(ϕ, θ, ψ)

* Based on SNAME notation

A. Preliminaries

Let $\{m\}$ denote a local Earth-fixed coordinate frame where the origin is fixed at the surface of the WGS-84 Earth ellipsoid, and the orientation is north-east-down (NED). Similarly, let $\{w\}$ denote a reference frame where the origin is fixed to, and translates with the water (due to current). The current is assumed irrotational, hence $\{w\}$ does not rotate relative to $\{m\}$. Recall that it is possible for a fluid traveling along a straight line to have vorticity, and similarly, for a fluid moving in a circle (or which changes direction) to be irrotational. The frame $\{b\}$ is a body-fixed frame where the axes coincide with the principal axes of the vehicle. The origin is located at the vehicle center of buoyancy. A general expression of the vehicle position can now be written as

$$\boldsymbol{p}^m_{mb} = \boldsymbol{p}^m_{mw} + \boldsymbol{R}^m_w \boldsymbol{p}^w_{wb}, \tag{1}$$

where $\boldsymbol{p}^m_{mb} \in \mathbb{R}^3$ is the position vector from $\{m\}$ to $\{b\}$, represented in $\{m\}$, and $\boldsymbol{R}^m_w \in SO(3)$ is the coordinate transformation matrix from $\{w\}$ to $\{m\}$. The velocity of $\{b\}$ relative to $\{m\}$, is given as $\boldsymbol{v}^m_{mb} := \dot{\boldsymbol{p}}^m_{mb}$, or decomposed in $\{b\}$ as $\boldsymbol{v}^b_{mb} := \boldsymbol{R}^b_m \boldsymbol{v}^m_{mb}$. The interpretation of the other variables follows directly. From (1) it follows that

$$\dot{\boldsymbol{p}}^m_{mb} = \dot{\boldsymbol{p}}^m_{mw} + \boldsymbol{R}^m_w \dot{\boldsymbol{p}}^w_{wb}, \tag{2}$$

where $\dot{\boldsymbol{R}}^m_w$ equals zero due to the assumption of irrotational current. Substituting for the derivatives, and pre-multiplying both sides of (2) with $\boldsymbol{R}^b_m$ gives the velocity relationship

$$\boldsymbol{v}^b_{mb} = \boldsymbol{R}^b_m \boldsymbol{v}^m_{mw} + \boldsymbol{v}^b_{wb}. \tag{3}$$

Analogous to the translational or linear velocities, their angular counterparts are given as $\boldsymbol{\omega}^m_{mb}$ and $\boldsymbol{\omega}^b_{mb} := \boldsymbol{R}^b_m \boldsymbol{\omega}^m_{mb}$.

For navigation purposes, two additional reference frames are common. The Earth-centered Earth-fixed (ECEF) frame is denoted $\{e\}$. The frame $\{l\}$ is a wander azimuth frame, defined such that it has zero angular velocity relative to the Earth about its z-axis. The initial orientation is NED and its origin is directly above the vehicle at the surface of the Earth ellipsoid. Note that $\{m\}$ is fixed relative to $\{e\}$, and that $\boldsymbol{R}^b_l \approx \boldsymbol{R}^b_m$ for limited geographical areas far from the poles. In light of the new frames, (3) may be restated as

$$\boldsymbol{v}^b_{eb} = \boldsymbol{R}^b_l \boldsymbol{v}^l_{ew} + \boldsymbol{v}^b_{wb}. \tag{4}$$

The correspondence between the variables above and the notation established by the Society of Naval Architects and Marine Engineers (SNAME) [14] is shown in Table I. Speed entities along the x-axis of $\{b\}$ are shown in Fig. 1.

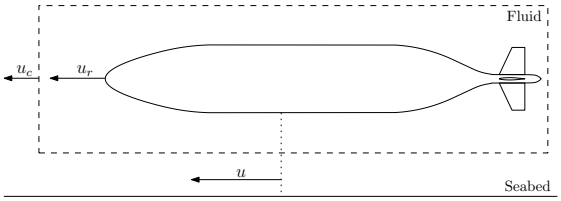

Fig. 1. Water-relative speed u_r, current speed u_c, and Earth-relative speed u, along the body x-axis. HUGIN 4500 AUV profile used for illustration.

B. Kinetic Vehicle Model

The HUGIN 4500 AUV is used as a case study in this work. The profile of the vehicle is outlined in Fig. 1. The bare hull is a body of revolution, and the cruciform tail fin configuration is top-bottom, port-starboard symmetric. A three degrees-of-freedom (3 DOF) model describing the vehicle motion in surge, sway and yaw, can be written as

$$\boldsymbol{M}_{RB}\dot{\boldsymbol{\nu}} + \boldsymbol{C}_{RB}(\boldsymbol{\nu})\boldsymbol{\nu} = \boldsymbol{\tau} - \boldsymbol{M}_A\dot{\boldsymbol{\nu}}_r - \boldsymbol{C}_A(\boldsymbol{\nu}_r)\boldsymbol{\nu}_r - \boldsymbol{d}(\boldsymbol{\nu}_r)\boldsymbol{\nu}_r - \boldsymbol{l}(\boldsymbol{\nu}_r) - \boldsymbol{g}(\boldsymbol{\Theta}). \tag{5}$$

A description and complete expressions of the different terms are given in [13]. The model in (5) was derived assuming negligible coupling from heave, roll, and pitch, which is a reasonable assumption for normal operations with the HUGIN 4500 AUV. The generalized velocities $\boldsymbol{\nu} = [u, v, r]^\top$ and $\boldsymbol{\nu}_r = [u_r, v_r, r]^\top$, denote generalized Earth-relative and generalized water-relative velocity, respectively. Since the current is irrotational by assumption, only the translational part of $\boldsymbol{\nu}$ and $\boldsymbol{\nu}_r$ differ. Recall the nomenclature in Table I.

For (5) one must decide upon using either $\boldsymbol{\nu}$ or $\boldsymbol{\nu}_r$ as the velocity state. As discussed in [13], a reasonable assumption at low vehicle angular rates or small current amplitudes is that $\dot{\boldsymbol{\nu}} \approx \dot{\boldsymbol{\nu}}_r$. This yields the final kinetic vehicle model

$$\boldsymbol{M}\dot{\boldsymbol{\nu}}_r = \boldsymbol{\tau} - \boldsymbol{c}(\boldsymbol{\nu}, \boldsymbol{\nu}_r) - \boldsymbol{d}(\boldsymbol{\nu}_r)\boldsymbol{\nu}_r - \boldsymbol{l}(\boldsymbol{\nu}_r) - \boldsymbol{g}(\boldsymbol{\Theta}), \tag{6}$$

where for simplicity we used $\boldsymbol{M} := \boldsymbol{M}_{RB} + \boldsymbol{M}_A$ and

$$\boldsymbol{c}(\boldsymbol{\nu}, \boldsymbol{\nu}_r) := \boldsymbol{C}_{RB}(\boldsymbol{\nu})\boldsymbol{\nu} + \boldsymbol{C}_A(\boldsymbol{\nu}_r)\boldsymbol{\nu}_r. \tag{7}$$

As seen from (7), the Coriolis and centripetal term $\boldsymbol{c}(\boldsymbol{\nu}, \boldsymbol{\nu}_r)$ depends on both $\boldsymbol{\nu}$ and $\boldsymbol{\nu}_r$. If there is no current then $\boldsymbol{\nu} = \boldsymbol{\nu}_r$. The linear Earth-relative velocity can be calculated from (4), which implies that the current should be measured or estimated. In the integrated navigation system studied herein, the current is included as a state in the Kalman filter (KF).

The model in (6) is a typical grey-box model where the vehicle motion is described by a set of ordinary differential equations (ODEs) with unknown parameters. With exception of propulsion coefficients obtained from open-water tests [15], the parameters were found from semi-empirical relationships and from experimental data collected by the HUGIN 4500. The parameter identification procedure was carried out using the methodologies reported in [13], [16].

A standard numerical ODE integration routine can now be used for solving (6) in order to recover the state. That is, model-based measurements of the water-relative velocity in surge and sway, as well as the yaw rate, can be attained from known actuation signals, attitude and current.

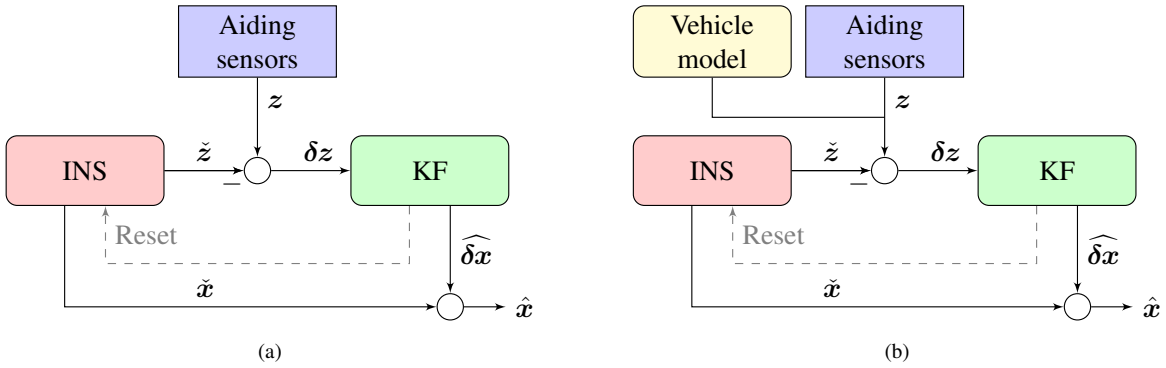

Fig. 2. High-level system outline. (a) Traditional aided INS. (b) Model-aided INS. The vehicle model is treated analogously to an external aiding sensor.

III. Model-Aided Underwater Navigation

Inertial measurement units, time of flight acoustics, velocity logs, and global positioning systems, are all common means for precision underwater navigation. As pointed out in [1], none of these techniques are perfect however, and a combination of them is usually employed in practice. This section reports the concept and development of an integrated model-aided INS, applied to underwater vehicle navigation.

A. Review of Traditional INS

The key components of any INS consist of an inertial measurement unit (IMU) and a set of navigation equations implemented in software. The equations take the gyro and accelerometer measurements from the IMU and integrate them to velocity, position and orientation. Due to inherent errors in the gyros and accelerometers, the INS navigation solution will have an unbounded drift, where the divergence rate depends on the quality of the IMU. One performance measure for an INS is given by its pure inertial drift in position, typically stated in nautical miles per hour (nmi/h). A good navigation grade INS drifts in the order of 1 nmi/h. Note that the pure inertial drift is not linear with time.

Since an INS is a diverging system, it requires an aiding system to bind the growth of its errors. Standard components such as compass and pressure sensor are usually included, where the latter effectively binds the vertical position drift, i.e. along the z-axis of $\{m\}$, or more precisely $\{l\}$. Navigation in the geographical horizontal plane is more complicated, and the main aiding methods to date involve time of flight acoustics, surface GPS, and DVL [1], [2]. The outline of a traditional aided INS is shown in Fig. 2(a), where the KF input is the difference between the output from the aiding sensor and the INS. The KF output includes estimates of the errors in the navigation equations, which are used for resetting the INS and for obtaining an enhanced estimate of the vehicle state; position, velocity and orientation. Besides modeling the INS errors, additional KF states may also be included, for instance colored noise in the aiding sensors.

B. Model-Aided INS

A DVL may or may not be part of the sensor suite, and even when it is, situations will occur where it fails to work or measurements are discarded due to decreased quality. As for the acoustic positioning, it may be available often or only sporadically. Both measurements are crucial for the INS performance, and as shown in [12] and Section IV-B herein, the solution from an INS without position and velocity aiding quickly becomes useless. This leads back to the question addressed in this work – can the output from a kinetic vehicle model improve the robustness and accuracy of an INS?

The basic idea and concept of using a kinetic vehicle model for aiding an INS is illustrated in Fig. 2(b), where the output from the model is treated analogously to that of an external aiding sensor. The model-aided INS clearly resembles the traditional INS in Fig. 2(a), and both systems may share many of the same aiding sensors. As implemented herein, the DVL in the traditional INS is merely replaced by the vehicle model, after doing necessary modifications in the KF. Note that the integration of a vehicle model in the navigation system does not require any additional instrumentation. As studied herein, the integration of kinetic models in underwater navigation systems is of particular interest for configurations lacking external velocity measurements. Other important implications involve systems (also having a DVL) where redundancy and integrity is important, e.g. during sensor dropouts or sensor failures, or emergency navigation. An aided INS utilizing both external velocity measurements and vehicle model output is subject to ongoing research.

A more detailed outline of the traditional and model-aided INS evaluated herein is shown in Fig. 3, differing only in the velocity aiding. The traditional INS aided with DVL and DGPS-USBL serves as the basis when later evaluating the performance of the model-aided INS in Section IV-B.

C. Measurement and Process Equations

A DVL measures the vehicle velocity relative to the bottom, and is therefore unaffected by current. In contrast, the velocity calculated by the kinetic vehicle model is relative to the water, hence to better make use of this velocity estimate for navigation purposes, the current must be accounted for.

In accordance to Fig. 2 and conventional KF notation, the general discrete input to the KF is given as

$$\boldsymbol{\delta z}_k = \boldsymbol{z}_k - \check{\boldsymbol{z}}_k, \tag{8}$$

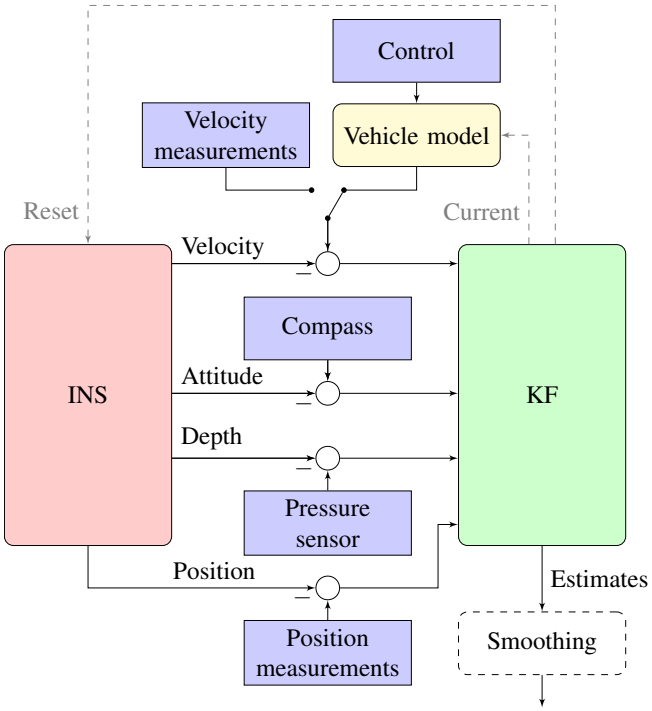

Fig. 3. Block diagram of model-aided (and traditional aided) INS. In this paper, external velocity measurements are not included while utilizing the output from the vehicle model, and the other way around when using external velocity measurements. This is illustrated with a switch. The position measurements may be available often or only sporadically.

where the accent $\check{(\cdot)}$ denotes a calculated variable, in this case from the INS. For the linear velocity we then get

$$\boldsymbol{\delta z}_{vel} = \boldsymbol{z}_{vel} - \check{\boldsymbol{z}}_{vel}, \tag{9}$$

where the time index is dropped for simplicity. As is standard for an INS, the velocity is $\check{\boldsymbol{z}}_{vel} = \check{\boldsymbol{v}}^l_{eb}$. The corresponding measurement is then $\boldsymbol{z}_{vel} = \tilde{\boldsymbol{v}}^l_{eb}$, where the accent $\tilde{(\cdot)}$ denotes a measured quantity. When utilizing the vehicle model output this is not the case, and the best we can do is to let

$$\boldsymbol{z}_{vel} := \check{\boldsymbol{v}}^l_{ew} + \check{\boldsymbol{R}}^l_b \check{\boldsymbol{v}}^b_{wb}, \tag{10}$$

which after substitution in (9) yields the expression

$$\boldsymbol{\delta z}_{vel} = \check{\boldsymbol{v}}^l_{ew} + \check{\boldsymbol{R}}^l_b \check{\boldsymbol{v}}^b_{wb} - \check{\boldsymbol{v}}^l_{eb}. \tag{11}$$

The definition in (10) clearly resembles the right hand side of (4), pre-multiplied with $\boldsymbol{R}^l_b$. The variables $\check{\boldsymbol{v}}^l_{eb}$ and $\check{\boldsymbol{R}}^l_b$ stem from the INS, $\check{\boldsymbol{v}}^b_{wb}$ is given by the vehicle model, and $\check{\boldsymbol{v}}^l_{ew}$ can for instance be calculated from empirical tide or current tables. If the current was measured it could be used in place of $\check{\boldsymbol{v}}^l_{ew}$. In this paper we assume that $\check{\boldsymbol{v}}^l_{ew} = \boldsymbol{0}$, which is to say that our best a-priori guess of the current is zero. It does not mean that the true current is zero. Note that the current is estimated in the KF. Also, since the model in (6) does not include the water-relative vehicle velocity in heave as a state, this model output is assumed to be zero. Similar to the current, the water-relative heave velocity is estimated in the KF. It is expected that the inclusion of a depth sensor in the navigation system renders this state observable.

A true variable is given as the sum of its calculated or measured value and a corresponding error, that is,

$$(\cdot) = \check{(\cdot)} + \delta(\cdot) \quad \text{and} \quad (\cdot) = \tilde{(\cdot)} - \delta(\cdot). \tag{12}$$

Replacing the current velocity and the vehicle model velocity in (11) with their errors and true values yields

$$\boldsymbol{\delta z}_{vel} = (\boldsymbol{v}^l_{ew} - \boldsymbol{\delta v}^l_{ew}) + \check{\boldsymbol{R}}^l_b(\boldsymbol{v}^b_{wb} - \boldsymbol{\delta v}^b_{wb}) - \check{\boldsymbol{v}}^l_{eb}, \tag{13}$$

which after some manipulation and first order approximations lead to the final expression for the measurement equation associated with the kinetic vehicle model output

$$\boldsymbol{\delta z}_{vel} = \boldsymbol{\delta v}^l_{eb} - \boldsymbol{S}(\check{\boldsymbol{v}}^l_{eb})\boldsymbol{e}^l_{lb} - \check{\boldsymbol{R}}^l_b \boldsymbol{\delta v}^b_{wb} - \boldsymbol{\delta v}^l_{ew}. \tag{14}$$

The variable $\boldsymbol{e}^l_{lb}$ is a measure of the calculation error in $\check{\boldsymbol{R}}^l_b$ and $\boldsymbol{S}(\cdot)$ is a skew-symmetric operator. The variables in (14) are all calculated by the INS or included in the KF process equation. Similar measurement equations as in (9) and (14) are also derived for the disparate aiding sensors in Fig. 3.

It is assumed herein that both the vehicle model output error $\boldsymbol{\delta v}^b_{wb}$ and the a-priori current prediction error $\boldsymbol{\delta v}^l_{ew}$ can be modeled as the sum of colored noise and zero-mean white noise. The entries of both $\boldsymbol{\delta v}^b_{wb}$ and $\boldsymbol{\delta v}^l_{ew}$ are considered uncorrelated. If we let $\boldsymbol{\Delta v}_{(\cdot)}$ and $\boldsymbol{\xi}_{(\cdot)}$ denote the colored and white noises, respectively, the errors can be expressed as

$$\boldsymbol{\delta v}^b_{wb} = \boldsymbol{\Delta v}^b_{wb} + \boldsymbol{\xi}_{v^b_{wb}} \tag{15}$$

$$\boldsymbol{\delta v}^l_{ew} = \boldsymbol{\Delta v}^l_{ew} + \boldsymbol{\xi}_{v^l_{ew}}. \tag{16}$$

While white noise is isolated in time, a colored process is local in time since its value at one instant also depends on prior values. Numerous correlation models can be used, depending on the studied noise characteristics [17], [18]. The colored noise in (15)-(16) is implemented as zero-mean first order Markov processes driven by white noise, that is,

$$\dot{\boldsymbol{\Delta v}}^b_{wb} = -\boldsymbol{T}^{-1}_{\boldsymbol{\Delta v}^b_{wb}} \boldsymbol{\Delta v}^b_{wb} + \boldsymbol{\gamma}_{\boldsymbol{\Delta v}^b_{wb}} \tag{17}$$

$$\dot{\boldsymbol{\Delta v}}^l_{ew} = -\boldsymbol{T}^{-1}_{\boldsymbol{\Delta v}^l_{ew}} \boldsymbol{\Delta v}^l_{ew} + \boldsymbol{\gamma}_{\boldsymbol{\Delta v}^l_{ew}}. \tag{18}$$

The colored noises are states in the KF process equation. Note that the KF estimate of $\boldsymbol{\Delta v}^l_{ew}$ is also an estimate of $\boldsymbol{\delta v}^l_{ew}$. This is again an estimate of the true current, since $\check{\boldsymbol{v}}^l_{ew}$ is zero by assumption, and consequently, $\boldsymbol{v}^l_{ew} = \boldsymbol{\delta v}^l_{ew}$.

The success of the Markov model relies on the determination of the parameters $\boldsymbol{T}_{(\cdot)}$ and the white noises $\boldsymbol{\gamma}_{(\cdot)}$. The matrices $\boldsymbol{T}_{(\cdot)}$ are diagonal with non-zero terms equal to the correlation time constants. As for $\boldsymbol{\gamma}_{(\cdot)}$ they are characterized by their standard deviations. Similarly for $\boldsymbol{\xi}_{(\cdot)}$ above. The desired standard deviations of $\boldsymbol{\Delta v}_{(\cdot)}$ may be used together with $\boldsymbol{T}_{(\cdot)}$ to find the steady-state standard deviations of $\boldsymbol{\gamma}_{(\cdot)}$.

D. Measurement and Process Noise Level Switching

The parameters describing the errors in the aiding sensors are time-invariant by default. For some sensors however, explicit knowledge of the measurement accuracy degradation or improvement from one sample to another may be available, e.g. through quality numbers reported by the sensor itself. If feasible, the quality of each single measurement should be sent to the KF in order to enhance the overall

Algorithm 1: Trajectory-based noise level switching

Input: Rudder deflection angle τ [deg]
Output: Adjusted KF noise characteristics for $\boldsymbol{\delta v}^b_{wb}$

if $|\tau| >$ *threshold* **then**
  adjust appropriate entries of $\boldsymbol{T}, \boldsymbol{\gamma}$ and $\boldsymbol{\xi}$
else
  t: time since $|\tau| >$ threshold
  if $t <$ *settle-time* **then**
    adjust appropriate entries of $\boldsymbol{T}, \boldsymbol{\gamma}, \boldsymbol{\xi}$
  else
    reset $\boldsymbol{T}, \boldsymbol{\gamma}, \boldsymbol{\xi}$ to nominal values
  end
end

navigation accuracy. Typically, the resulting effect is an increase or decrease in the measurement white noise, and in some cases, a change in the standard deviation or correlation time constant for the colored noise. In this work, the position measurements in Fig. 3 are accompanied by distinct quality measures for each sample, as reported by the sensor.

Analogous to a conventional aiding sensor, the vehicle model output varies in quality. In particular, the accuracy during tight turning maneuvers is slightly lower than for steady forward motion, as experimentally validated in [13]. In [19], the normalized innovation is monitored in order to detect a maneuver, and if it exceeds a certain threshold the KF process noise is adjusted. A related approach is applied in this paper for adjusting the process and measurement noise characteristics associated with the vehicle model output error $\boldsymbol{\delta v}^b_{wb}$. In contrast to the systems in [19], a maneuver for an underwater vehicle is detected directly from measured actuation. This knowledge may be used for establishing a noise level switching rule. An outline of the rule used in this paper is given in Algorithm 1. While not considered in this work, a similar criterion can easily be developed for stern plane deflections and vertical maneuvers.

IV. Experimental Evaluation

The model-aided INS was implemented and experimentally evaluated using data collected by the HUGIN 4500 AUV, a field-deployed AUV designed for underwater surveying and mapping. An overview of the experimental setup is given subsequently, followed by experimental results.

A. Experimental Setup

1) Vehicle Description: HUGIN 4500 is the latest member of the Kongsberg Maritime HUGIN AUV family. Figure 4 shows a picture from one of the sea-trials in October 2006. The diameter and length of the vehicle are 1 and 6.5 meters, respectively. The vehicle can operate for 60-70 hours at depths down to 4500 meters, at a cruising speed of about 3.7 knots. The vehicle is passively stable in roll and close to neutrally buoyant. For propulsion, it is fitted with a single three-bladed propeller. A cruciform tail configuration with four identical control surfaces is used for maneuvering.

Fig. 4. The HUGIN 4500 AUV prior to sea-trial launch in October 2006.

TABLE II
IMU SPECIFICATIONS

Model	Gyro Technology	Gyro Bias	Accelerometer Bias
IXSEA IMU90	Fiber optic	$\pm 0.05^\circ$/h	$\pm 500\ \mu g$

TABLE III
PRIMARY NAVIGATION AIDING SENSORS

Variable	Sensor	Precision	Rate
Position	Kongsberg HiPAP	Range, Angle: < 20 cm, 0.12°	Varying*
Velocity	RDI 300kHz DVL	$\pm 0.4\,\% \pm 0.2$ cm/s	1 Hz
Pressure	Paroscientific	0.01 % full scale	1 Hz

* Approximately 1/3 Hz. In real-time position updates are received at about 1/30 Hz, from the surface vessel via an acoustic link.

HUGIN 4500 is equipped with a traditional aided INS, as shown in Fig. 3. Some IMU specifications are listed in Table II. A surface ship tracks the AUV with an USBL acoustic positioning system. By combining DGPS with USBL, a global position estimate can be obtained, which is then transmitted to the AUV. Additional navigation sensors include compass, pressure sensor, and DVL. Primary aiding sensors and some of their specifications are listed in Table III. For additional information on the navigation system and the navigation system accuracy, the reader is referred to [2], [20], [21].

2) Experimental Description: In September and October 2006, several sea-trials were conducted with HUGIN 4500 in the vicinity of 59° 29' N, 10° 28' E, in the Oslo-fjord, Norway. Roughly 60 hours of data were collected, of which a subset of about 3.5 hours is utilized in this paper. In the first part, the vehicle was kept at a constant depth while moving along square-shaped trajectories, as described in [16]. In the second part, the vehicle followed a standard lawn-mover pattern, typical for a survey AUV. The trajectory corresponding to this data is shown in Fig. 5.

3) Data Post-Processing: The position measurements were wild-point filtered prior to being utilized in this paper. The HUGIN navigation system then re-processed the appropriate sensor data to get real-time estimates from the KF (this is done using a copy of the at-sea navigation system). The traditional INS with sensor specifications described in Section IV-A.1 serves as the basis or ground truth when evaluating the performance of the model-aided INS. The basis solution was smoothed in order to enhance accuracy,

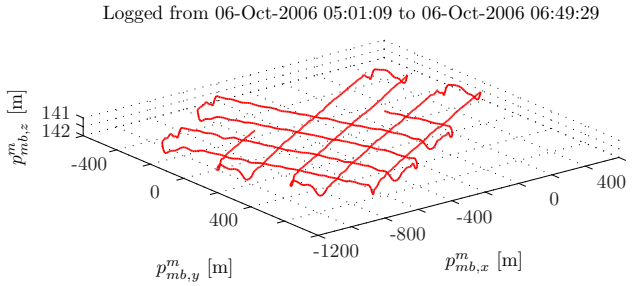

Fig. 5. Three dimensional vehicle lawn-mower trajectory. The trajectory shows the smoothed local position, which is considered as ground truth.

which for the vehicle position was estimated to be 0.75 meters (1σ) in north and east. In general, this accuracy partly depends on the GPS on the surface ship. Both the experimentally proven accuracy of the navigation system and the post-processing steps are thoroughly described in [21].

B. Experimental Results

This section evaluates the performance of the model-aided INS described in Section III. With exception of the parameters associated with the vehicle model, all the KF tuning parameters are identical for the traditional and model-aided INS. Unless mentioned otherwise, the position measurements are received regularly at about 1/3 Hz.

1) Estimation of sea current and vehicle model output error in model-aided INS: Since the heave velocity from the vehicle model is zero, it follows from (12) that the KF estimate of $\delta v^b_{wb,z}$ is also an estimate of $v^b_{wb,z}$. The estimated heave velocity corresponding to square 3 in Table IV is shown in Fig. 6. Similar results were obtained for the other subsets of data as well. The good observability is due to the inclusion of a depth sensor in the sensor suit. The model-aided INS also estimates the x and y components of $\boldsymbol{\delta v}^b_{wb}$. Both were found to be less than 1 cm/s throughout.

For the estimated current, the magnitude is the Euclidian norm of $\boldsymbol{\delta v}^l_{ew}$, given in m/s. In this work it is assumed that the vertical current, or equally, the third entry of $\boldsymbol{\delta v}^l_{ew}$ is negligible. Recall that the estimate of $\boldsymbol{\delta v}^l_{ew}$ is also an estimate of $\boldsymbol{v}^l_{ew}$. The current direction β_w is calculated from

$$\beta_w = \operatorname{atan2}\left(\delta v^l_{ew,y}, \delta v^l_{ew,x}\right), \tag{19}$$

where $\beta_w \in [0, 360)$ is relative north with positive rotation clockwise, i.e. $\beta_w = 90$ degrees yields east direction. The estimated current magnitudes and directions from four distinct square maneuvers are summarized in Table IV. The estimates from the model-aided INS are compared to the least-squares (LS) results reported in [16]. The two different approaches show good agreement. The KF evolutions for square 3 and 4 are shown together with the corresponding LS solutions in Fig. 7. The model-aided INS values in Table IV are taken as the median of the last 8 minutes of the KF time sequences.

2) Position measurement dropout in traditional and model-aided INS: This experiment was done in order to evaluate the performance of the model-aided and traditional INS (without external velocity aiding), in the case where position measurements for some reason become unavailable.

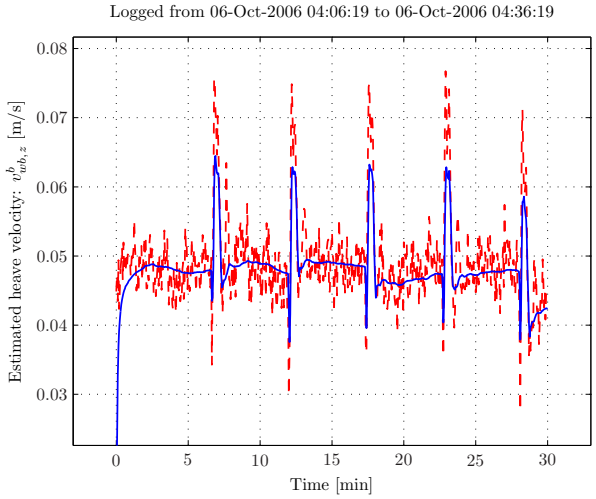

Fig. 6. Estimated vehicle water-relative heave velocity for square 3. The blue (solid) is the estimate of $v^b_{wb,z}$ and the red (dashed) is the basis $v^b_{eb,z}$. From (4) it is straightforward to verify that $v^b_{eb,z}$ and $v^b_{wb,z}$ are approximately equal for zero vertical current and small roll and pitch angles.

TABLE IV
SEA CURRENT ESTIMATION DURING SQUARE MANEUVERS

Square	Estimation approach	Log time	RPM	$\|\boldsymbol{v}^l_{ew}\|$	β_w
1	Least-squares	Oct 06 @ 02:06-02:20	165	0.015	17.2
	Model-aided INS	Oct 06 @ 02:02-02:22	165	0.013	27.2
2	Least-squares	Oct 06 @ 03:01-03:21	165	0.018	305.5
	Model-aided INS	Oct 06 @ 03:01-03:21	165	0.016	318.4
3	Least-squares	Oct 06 @ 04:15-04:34	165	0.004	301.7
	Model-aided INS	Oct 06 @ 04:06-04:36	165	0.004	310.0
4	Least-squares	Oct 06 @ 07:31-07:46	165	0.021	162.7
	Model-aided INS	Oct 06 @ 07:26-07:48	165	0.022	156.0

The scenario is best illustrated in Fig. 8(a), where the real-time KF receives regular position measurements for about 62 minutes. The position aiding is then disabled for 30 minutes, before again being enabled for the remainder of the survey.

When aided with high frequency DGPS-USBL, the model-aided and traditional INS are found to perform comparably in terms of calculated position errors, which is the difference between the local basis position and the local position estimated by the real-time navigation system under consideration. The position covariance estimated by the model-aided INS is found to be more reliable and slightly lower than for the traditional INS. This is discussed in more detail in [12]. For the part without position aiding, the traditional INS breaks down quickly, as can be seen in Fig. 8(b) where the maximum horizontal position error is 961 meters. The model-aided INS continues to perform excellently, and the maximum horizontal position error is 6 meters. From Fig. 8(d) the errors can be seen to be within one standard deviation (1σ). The estimated trajectory is shown in Fig. 8(c), closely following the basis data. Overall the model-aided INS performs very well, and superior to the traditional INS without velocity and position aiding. In general, the performance of the traditional INS without velocity aiding rapidly degrades with decreasing position measurement update frequency. On the contrary, the model-aided INS is more robust to the position update frequency.

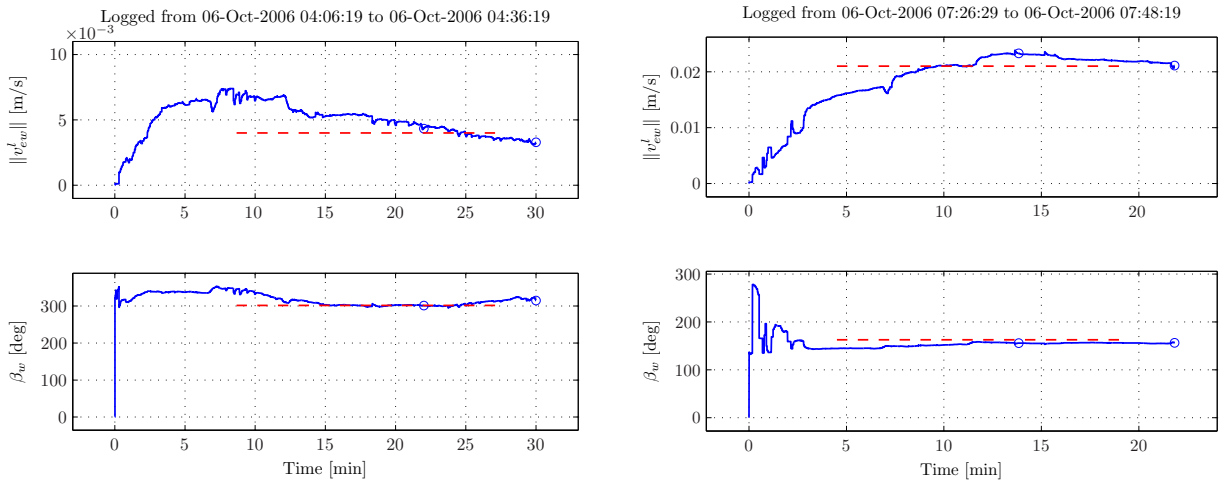

(a) (b)

Fig. 7. Estimated current using LS and model-aided INS: (a) Estimated current for square 3 in Table IV. The model-aided real-time KF estimates are shown in blue (solid). The red (dashed) lines are the corresponding LS solutions. (b) Estimated current for square 4 in Table IV. Similar labels as in (a). The model-aided INS values in Table IV are taken as the median of the last 8 minutes of the KF estimates. The intervals are indicated with blue (o).

C. Discussion of Results

It should be pointed out that the navigation accuracy obtained during time slots without position aiding is limited to the accuracy of the KF estimated current and vehicle model output error. In particular, if the current does not vary significantly throughout the time period where position measurements are absent, the navigation accuracy will remain good. The importance of distinguishing between the vehicle model output error and sea current is also emphasized, and as is apparent from (14), an error represented in $\{b\}$ is distributed to $\{l\}$ through the transformation matrix $\boldsymbol{R}_b^l$. Unless accounted for, an error in the vehicle model output will result in a time varying error in the current estimate. Depending on the size of the model output error, the effect will be easily visible before and after large course changes. Finally note the capability of estimating the current may be of interest for oceanographic research. Another interesting example includes autonomous mission planning [22].

V. Conclusions

This paper reports the development of a complete model-aided INS for underwater vehicle navigation. The navigation system is novel in that an accurate model of the vehicle dynamics is utilized for aiding the INS, and the navigation performance is experimentally evaluated using real AUV data. The system accommodates simultaneous estimation of vehicle model output errors and current. The estimated current shows good agreement with an earlier reported LS solution. It is found that the error in the model-aided INS position estimate is significantly lower than that of the traditional INS throughout time segments where position and velocity measurements are absent. The model-aided INS also performs equally well or better than the traditional INS (without velocity aiding) in cases with regular position updates. The difference in performance increases with decreasing position update rate. The experimental results demonstrate that it is possible to considerably improve the accuracy and robustness of an INS by utilizing the output from a kinetic vehicle model. The proposed navigation system does not require any additional instrumentation. To the best of our knowledge, the results are the first report on the implementation and experimental evaluation of a complete model-aided INS for underwater vehicle navigation. The proposed approach shows promise to improve navigation capabilities both for systems lacking disparate velocity measurements, and for systems where redundancy and integrity is important.

References

[1] J. C. Kinsey, R. M. Eustice, and L. L. Whitcomb, "A survey of underwater vehicle navigation: Recent advances and new challenges," in *Proceedings of the 7th IFAC Conference of Manoeuvring and Control of Marine Craft (MCMC)*, Lisbon, Portugal, 2006.

[2] B. Jalving, K. Gade, O. Hagen, and K. Vestgård, "A toolbox of aiding techniques for the HUGIN AUV integrated inertial navigation system," in *Proceedings of the MTS/IEEE Oceans Conference and Exhibition*, vol. 2, San Diego, CA, 2003, pp. 1146–1153.

[3] B. Jalving, K. Gade, K. Svartveit, A. Willumsen, and R. Sørhagen, "DVL velocity aiding in the HUGIN 1000 integrated inertial navigation system," *Modeling, Identification and Control*, vol. 25, no. 4, pp. 223–235, 2004.

[4] M. B. Larsen, "High performance doppler-inertial navigation-experimental results," in *Proceedings of the MTS/IEEE Oceans Conference and Exhibition*, vol. 2, Providence, RI, 2000, pp. 1449–1456.

[5] A. Gadre and D. Stilwell, "A complete solution to underwater navigation in the presence of unknown currents based on range measurements from a single location," in *Proceedings of the IEEE/RSJ International Conference on Intelligent Robots and Systems*, Edmonton, Canada, 2005, pp. 1420–1425.

[6] J. Jouffroy and J. Opderbecke, "Underwater vehicle trajectory estimation using contracting PDE-based observers," in *Proceedings of the American Control Conference*, Boston, MA, 2004, pp. 4108–4113.

[7] J. C. Kinsey and L. L. Whitcomb, "Model-based nonlinear observers for underwater vehicle navigation: Theory and preliminary experiments," in *Proceedings of the IEEE International Conference on Robotics and Automation (ICRA)*, Rome, Italy, 2007, pp. 4251–4256.

[8] J. E. Refsnes, A. J. Sørensen, and K. Y. Pettersen, "A 6 DOF nonlinear observer for AUVs with experimental results," in *Proceedings of the 15th IEEE Mediterranean Conference on Control and Automation (MED)*, Athens, Greece, 2007.

[9] M. Bryson and S. Sukkarieh, "Vehicle model aided inertial navigation for a UAV using low-cost sensors," in *Australasian Conference on Robotics and Automation*, Canberra, Australia, 2004.

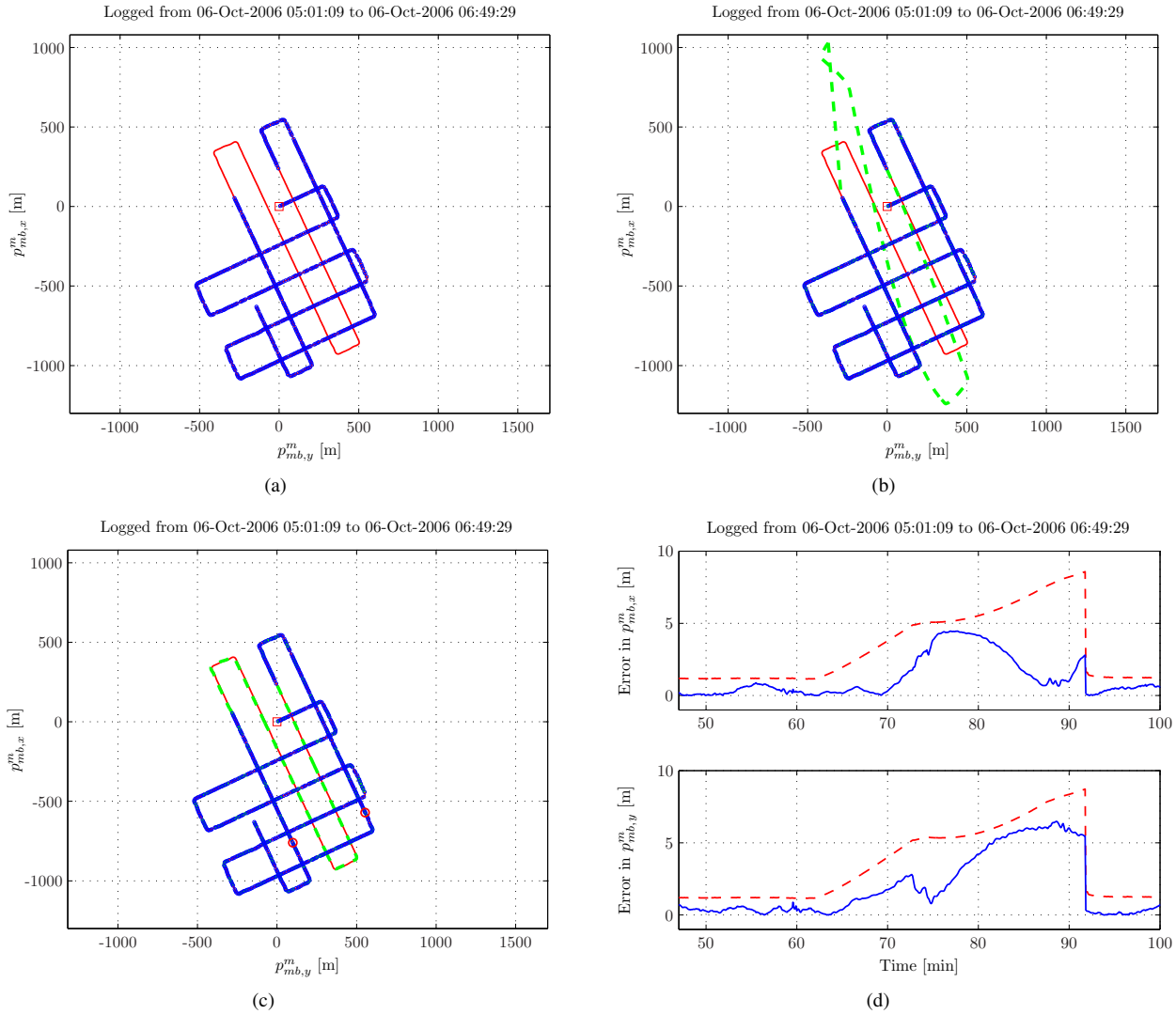

Fig. 8. Performance of traditional and model-aided INS during position measurement dropout: (a) The red (solid) trajectory is the two dimensional local basis position. The red square shows the initial position used in the KF. The blue (o) data show wild-point filtered position measurements logged at about 1/3 Hz. The segment without position measurements corresponds to 30 minutes. (b) Real-time navigation solution obtained with traditional INS shown in green (dashed). Other data as before. The system shows poor performance without position measurements. (c) Real-time navigation solution obtained with model-aided INS shown in green (dashed). Other data as before. The system shows excellent performance, also without position measurements. The circles (red) indicate 47 and 100 minutes into the run. (d) The position errors (assuming basis is correct) for the model-aided INS in north and east are shown in blue (solid). The corresponding estimated real-time KF position uncertainties (1σ) are shown in red (dashed).

[10] M. Koifman and I. Bar-Itzhack, "Inertial navigation system aided by aircraft dynamics," *IEEE Transactions on Control Systems Technology*, vol. 7, no. 4, pp. 487–493, 1999.

[11] J. F. Vasconcelos, C. Silvestre, and P. Oliveira, "Embedded vehicle dynamics and LASER aiding techniques for inertial navigation systems," in *Proceedings of the AIAA Guidance, Navigation, and Control Conference*, Keystone, CO, Aug. 2006, pp. 4025–4047.

[12] Ø. Hegrenæs, O. Hallingstad, and K. Gade, "Towards model-aided navigation of underwater vehicles," in *Proceedings of the 15th International Symposium on Unmanned Untethered Submersible Technology (UUST)*, Durham, NH, Aug. 2007.

[13] Ø. Hegrenæs, O. Hallingstad, and B. Jalving, "A comparison of mathematical models for the HUGIN 4500 AUV based on experimental data," in *Proceedings of the IEEE International Symposium on Underwater Technology (UT)*, Tokyo, Japan, 2007, pp. 558–567.

[14] SNAME, "Nomenclature for treating the motion of a submerged body through a fluid," The Society of Naval Architects and Marine Engineers, Tech. Rep. Technical and Research Bulletin No. 1-5, 1950.

[15] Ø. Hegrenæs, "Open-water propulsion test using full-scale propellers for the HUGIN AUV family," University Graduate Center, Kjeller, Norway, Tech. Rep., 2006.

[16] Ø. Hegrenæs, O. Hallingstad, and B. Jalving, "A framework for obtaining steady-state maneuvering characteristics of underwater vehicles using sea-trial data," in *Proceedings of the 15th IEEE Mediterranean Conference on Control and Automation (MED)*, Athens, Greece, 2007.

[17] A. Gelb, *Applied Optimal Estimation*. The MIT Press, 1974.

[18] X. R. Li and V. P. Jilkov, "Survey of maneuvering target tracking. Part I: Dynamic models," *IEEE Transactions on Aerospace and Electronic Systems*, vol. 39, no. 4, pp. 1333–64, Oct. 2003.

[19] Y. Bar-Shalom, X. R. Li, and T. Kirubarajan, *Estimation with Applications to Tracking and Navigation*. John Wiley & Sons, 2001.

[20] B. Jalving, K. Vestgård, and N. Størkersen, "Detailed seabed surveys with AUVs," in *Technology and Applications of Autonomous Underwater Vehicles*, G. Griffiths, Ed. Taylor & Francis, 2003, vol. 2, pp. 179–201.

[21] K. Gade, "NavLab, a generic simulation and post-processing tool for navigation," *European Journal of Navigation*, vol. 2, no. 4, pp. 21–59, Nov. 2004, (see also http://www.navlab.net/).

[22] P. E. Hagen, Ø. Midtgaard, and Ø. Hasvold, "Making AUVs truly autonomous," in *Proceedings of the MTS/IEEE Oceans Conference and Exhibition*, Vancouver, Canada, 2007.